

Master Thesis

Master of Energy Engineering

Optimization of an offshore wind electrical collection system

Memoria

September 14, 2022

Author: Bernardo Castro Valerio

Director: Oriol Gomis-Bellmunt

Academic year: 2021-2022



Escola Tècnica Superior
d'Enginyeria Industrial de Barcelona

ETSEIB 

The large, light blue 'ETSEIB' text is positioned at the bottom of the page. To its right is the UPC logo, which consists of a blue circle containing a white grid of dots and the letters 'UPC' below it.

Contents

Abstract	4
1 Introduction	5
1.1 Thesis Objective	5
1.2 Environmental Impact	5
1.3 Planning and scope of the project	6
2 Fundamentals	7
2.1 Previous Research	7
2.2 Offshore Wind Power Plants	7
2.2.1 Submarine cables	9
2.3 Electrical model	10
2.3.1 Resistance	11
2.3.2 Reactance	12
2.3.3 Shunt Capacitance	12
2.3.4 Ybus matrix	12
2.4 Power flow analysis	12
2.4.1 Per unit system	14
2.5 Cost Models	14
2.5.1 Cable Cost	14
2.5.2 Energy Loss Cost	15
2.6 Graph theory	16
2.7 Optimization model	16
3 Design tool description	18
3.1 Algorithms	18
3.2 Limitations	19
4 Case Study	22
4.1 Input Data	22
4.1.1 Farm layout	22
4.2 Layout distribution	23
4.3 Combination of cable diameters	24
4.4 Optimal distribution analysis	27
5 Analysis of the performance of the design tool	29
5.1 Performance of DT in solving case study	29
5.2 Sensibility analysis	31
Conclusion	35
References	36
A Substation positioning	38
B Increased number of possible collection system	40
C Increased allowed distance between turbines	41

List of Figures

1	Radial system [16]	8
2	Radial Loop system [16]	8
3	AC Star system [16]	9
4	Cable types [17]	10
5	Lumped circuit model (π -circuit) of a transmission line between nodes k and m	11
6	Single-line diagram of one feeder string [21]	12
7	Basic type of graphs [26]	16
8	Pareto Front [28]	17
9	Algorithm to calculate the total distance of all viable cable layouts	20
10	Algorithm for cable diameter decision	21
11	OWWP layout represented in a graph	23
12	Least distance set up for cable distribution	23
13	Subsequent layout distributions	24
14	Combination distribution on a comparison of Energy loss cost and cable installation cost	25
15	Pareto Front of combinations	25
16	Pareto Front analysis	26
17	Cable diameter installment	27
18	Box and whiskers plot representing the different Pareto front cost distribution	28
19	Node voltage in each turbine node.	28
20	Number of results generated with increasing number of possible connections	30
21	Time taken to undergo section 3 of the DT over increasing possible connections	30
22	Time taken to undergo section 3 of the DT over increasing possible connections	31
23	Box and whiskers plot representing the different Pareto front cost distribution	32
24	Comparison of shift in energy and cable related costs	32
25	Box and whiskers plot with the iterations in change of LCoE used to simulate for cable related costs	33
26	Box and whiskers plot with the iterations in change of LCoE used to simulate for energy related costs	33
27	Total cost comparisons	34
28	OWWP layout represented in a graph	38
29	Least distance set up for cable distribution	39
30	Cable possibilities with possible connections equal to 14	40
31	Solution of layout with increased possible connections	40
32	Cable possibilities with maximum allowed cabling distance equal to 15D	41

List of Tables

1	Literature review summary	7
2	Cable information obtained from ABB XPLE Cables [17]	10
3	Cable transport and installation cost data [k€/km] [24]	15
4	Economic Parameters based on [25]	15
5	Sections of the DT	18
6	Inputs considered for case study	22
7	Minimum cable per section position	24
8	Anchor and Utopia point	26
9	Time ditribution in running the DT	29

Abstract

Onshore wind energy production locations are every day diminishing more and more. Resulting in a transition to offshore projects. With new benefits and challenges that need to be tackled. One of them is the optimization of the infield collection system. This work presents the description, results and analysis of a design tool that has two main objectives; the layout of the cables and the diameter of such.

The work presents the state of the art of solutions present with such as minimum spanning tree, genetic algorithms and other graph based solutions. Covering a review of offshore wind power plants, infield distributions and industrial submarine cables. As well as explaining the mathematical theory and electrical theory required to understand power flow analysis by using the Newton-Raphson method. Furthermore describing the optimization process through Pareto search algorithm and the cost models utilized.

Utilizing the theory presented a design tool was coded in Matlab 2021b and the main two algorithms are drawn and described. Decomposing them in a total six steps with the required user inputs for them. In addition, the limitations and reach of the working code are explained. A case study is presented of a power plant consisting of twenty four 7 kW turbines in a 4 x 6 arrangement. Where the results are graphically presented and further analysed. Presenting an optimal layout distribution, that utilizes six different cable diameters.

Lastly, a performance analysis was conducted on the design tool. Where variables such as the possible cable connections and cost of electricity were altered. Showing an exponential increase on time and a sensitivity analysis respectively.

1 Introduction

With a total of 4,95 MW power capacity, in 1991, the first offshore wind farm was installed in Vindeby, Denmark [1]. This project had 11 wind turbines with a 35 m rotor diameter, creating an output capacity of 450 kW each. Such project might be decommissioned since 2017, however, it is recognized as a starting point of now a booming sector in the energy industry. Where Siemens now a day produces turbines with 222 m diameter with an output of 14 MW, with energy capacity 31 times higher than those in Vindeby [1].

The European commission estimated that up to 450GW of OWPP installations could be needed by 2050 [2]. In today's energetic climate, there is only 20 GW of offshore wind energy operating in Europe, making the leap from 20 GW to 450 GW will need a visionary leap. An Offshore wind power plant (OWPP) is defined as a large formation of wind turbines located offshore. The turbines are situated in poles or floating structures. Advantages of an OWPP over an onshore wind power plant include having a higher energy production potential due to higher and more steady winds [3], not being as Geo-location dependent as onshore plants and lower installation restrictions allow for larger wind turbines.

On the other hand, moving from onshore to offshore has some disadvantages. For instance, the cabling distance increases such that it can be involved to be 9% of the total cost [4].

1.1 Thesis Objective

The objective of this work is to create and implement a DT that generates, calculates and evaluates possible branch interconnection arrays in an OWPP. Creating the possible array with input settings of maximum cabling distance allowed between turbines, maximum cabling distance towards the substation, number of connections allowed in the substation. Secondly, calculating the euclidean distance of the whole cabling system. To evaluate the interconnection arrays with smallest total distance with a multi-objective function to determine the cable diameter of such connections.

1.2 Environmental Impact

This work does not entail significant direct environmental impacts. Nevertheless, if the design tool (DT) were to be used in future projects, impacts derived from such projects are described in this section.

In order to adequately protect the cables from all forms of hostile seabed intervention cable burial and other protection methods are used. These interventions include can arise from, but not limited to, becoming entangled by seabed deployed fishing or engaged by an otter board. OWPP cables are targeted to be buried between one and two meters by using ploughs, sleds or burial machines [5]. The seabed and sediment disturbance can have dispersion footprints extending up to 9 km. Resulting in collateral environmental impacts that need to be addressed and mitigated.

Potentially significant effects are described as seabed disturbance and increase in suspended sediment concentrations. In addition, other effects also include: potential contaminant release, electro-magnetic effects, heating effects and cable coating effects. However, studies have shown that following seabed disturbances, initial recolonisation takes place rapidly following a disturbance event.

Mitigation activities in sensitive locations are proposed, consisting of altering cable route, exclusion zones and micro-siting are tackled in an environmental report on a project to project basis. [5]

1.3 Planning and scope of the project

The project is focused on the medium voltage infield collection system of an offshore OWPP. Where considerations have been taken into account. The first restriction is that each turbine node can only have a maximum of one entry and one exit cable. Secondly, there are no crossing of cables allowed in the the interconnection array. Thirdly, for the evaluation of cable diameter the two parameters taken into account is the installation cost of the cable and the energy lost cost.

The DT is set out to be coded in MATLAB in order to use some pre-set libraries such as graph theory and financial libraries. This work will not only focus on completing the thesis objective presented above, but also in evaluating its sensitivity to price changes and evaluating the efficiency of completion of the objective.

The written work is divided in five chapters. Following this introduction, chapter 2 being the theoretical and data fundamentals needed for the creation of the DT. Covering previous research, elements of an OWPP, infield configurations, electrical design, and optimization methods. Continued by the description of the DT methodology in chapter 3. Continuing with chapter 4, where the DT is implemented in a case study, the results are presented and analysed. The 5th chapter is focused with the scrutiny of the program and its behaviour to changes in input variables. Followed by a conclusion of the project at the end.

2 Fundamentals

2.1 Previous Research

With the increasing development and investment in OWPP there are already existing tools and investigations on the optimization of the infield collection system. In this section a summary and recollection of such will be described.

Starting with available software tools, there are some that are capable of performing at least part of the task involved. These are *WindPro*, *EeFarm*, and *TopFarm*. Where factors, such as turbine cost, wake effect operation and maintenance are taken into account [6]. For example, *WindPro* optimizes the layout using data such as turbine spacing, setback distances and noise level, In addition, is able to perform electrical design such as load flow, cable loss, voltage fluctuations.

When covering the literature review, there are two main aspects to cover. The optimization of the cable layout, and the optimization of the cable diameter. For the first problem, previous works cover the use of greedy algorithms such as : Minimum spanning tree problem, Ant colony algorithm, Minimum salesman problem; as well as Genetic algorithm and Particle Swarm optimization between others. On the other hand, for the determination of the cable diameters, works were found to cover the use of Multi objective function and Genetic algorithms. Table 1 shows a summary of the different works read previous to the creation of this paper.

Table 1: Literature review summary

Algorithm	Cable layout	Cable diameter
Minimum Spanning tree	[7], [8]	
Ant colony	[9]	
Travelling sales man problem	[10],[11]	
Particle swarm optimization	[12]	
Genetic algorithm	[11]	[13]
Modified bat algorithm		[10]
Multi Objective Function		[14]

From this literature review it is important to note that any DT created on forward should try to cover the following [15] :

- a) DT should aim to reduce computational cost.
- b) No cross lay out should be permitted.
- c) Current in each cable under full load condition should not exceed the selected cable current capacity.

2.2 Offshore Wind Power Plants

The electrical system for an OWPP can be described in two sections [16]. The infield collection system that connects all the turbines to each other and the substations. And the second the one that connects the OWPP to the onshore grid, with usually higher voltage and refereed as the transmission system. The collection system may collect power in AC or DC. This work, will be focused sorely on a AC collection system. Which topologies can be describes as follows [16]:

1) Radial Collection Radial collection several turbines are connected to a common cable depending on the current capacity. Additionally, several radials or strings are connected to together in the substation that collects the power of the entire power plant.

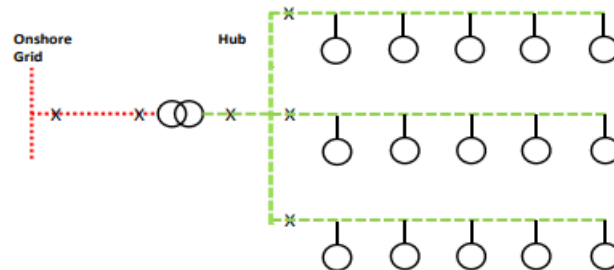


Figure 1: Radial system [16]

2) Radial-loop collection In Radial-loop collection there exist a higher reliability than in radial collection, as a radial loop can be reconfigured in case of faults. On the other hand, the system requires a higher level of control and initial investment due to the increased length of cable and reconfiguration switches (shown in figure 2 as red x). During normal operation such switches are in open state.

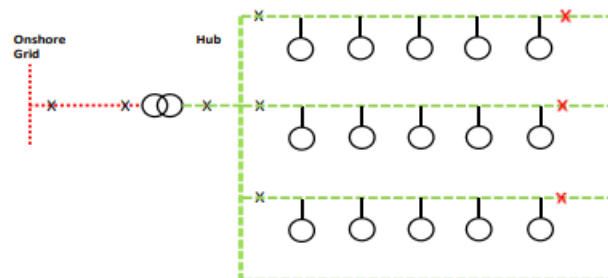


Figure 2: Radial Loop system [16]

3) AC Star/cluster collection In a star configuration each turbine is grouped and connected in a point of interconnection. The cluster depends on the current capacity of the main cable similar to the radial collection system. However, the current in this collection system does not vary on each collection point of a turbine, but is equal to the combination of all the currents in the cluster.

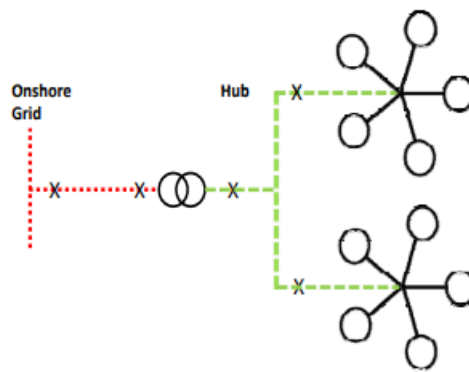


Figure 3: AC Star system [16]

In addition to the AC collection systems presented above, in OWPP there are also proposals to have medium voltage DC infield collection systems. The purpose of such systems is to gain advantages in terms of efficiency and eliminate the need of large converter stations offshore. Topologies include: DC radial system, DC series/daisy chain connection and DC series-parallel connection.

In the AC system, the collection system designs mostly use 33kV AC for collection. This is dictated mostly by the ready availability of switch gear and protection equipment for that voltage range [16].

2.2.1 Submarine cables

In OWPP installations three-core subsea cables with solid insulation are typically used for operation voltages up to 132 kV [5], such as: Ethylene Propylene Rubber (ERP) or most commonly Cross-linked polyethylene (XLPE) [6]. This is due to low losses, high reliability and low ecological impact. The core of the cable can be either copper or aluminum, with the latter being the least common due to lower current capacities. XLPE cable losses are primarily due to ohmic losses in the conductor and metallic screen, but can be loaded continuously to a temperature of 90°C [17]. There are two types of core settings which are explained as follows and shown in figure 4.

Single-core: Can be laid separated or close, with close laying resulting in lower losses. A separate installation will result in a reduction of mutual heating but higher armour losses. To reduce this they have non-magnetic armour.

Three-core: There is little or no coupling between the phases and therefore, the system remains symmetrical. In addition, the cabling is laid in one instance, differing to single-core that requires separate installation, thus reducing the installation cost [6].

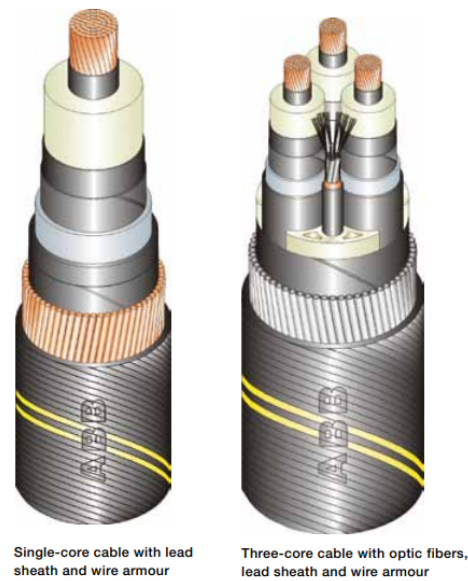


Figure 4: Cable types [17]

For this thesis, three-core ABB XPLE cables are used , which data is shown in table 2.

Table 2: Cable information obtained from ABB XPLE Cables [17]

Cross section	diameter	Inductance	Capacitance	Current	Diameter over insulation
mm^2	mm	mH/km	$\mu F/km$	A	mm
95	11,2	0,44	0,18	300	29,6
120	12,6	0,42	0,19	340	31
150	14,2	0,41	0,21	375	32,6
185	15,8	0,39	0,22	420	34,2
240	18,1	0,38	0,24	480	36,5
300	20,4	0,36	0,26	530	38,8
400	23,2	0,35	0,29	590	41,6
500	26,2	0,34	0,32	655	45
630	29,8	0,32	0,35	712	48,6
800	33,7	0,31	0,38	775	52,5

2.3 Electrical model

The transmission lines between turbines lumped-circuit equivalent is modeled as a π -equivalent circuit such as [18] and shown in figure 5

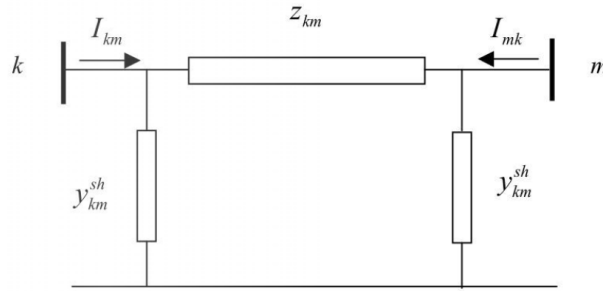


Figure 5: Lumped circuit model (π -circuit) of a transmission line between nodes k and m

Such that the impedance Z_{k-m} and shunt capacitance Y_{k-m} are:

$$Z_{k-m} = R_{k-m} + jX_{k-m} \quad (1)$$

$$Y_{k-m}^{sh} = G_{k-m}^{sh} + jB_{k-m}^{sh} \quad (2)$$

Where R_{k-m} is the series resistance, X_{k-m} the series reactance, the shunt conductance and B_{k-m} the shunt susceptance. The shunt capacitance is assumed to be symmetrical on both sides.

2.3.1 Resistance

The resistance of the XLPE cable is to be calculated according to the IEC 60287-1-1 standard [19] by the following equation:

$$R_{AC} = R_{dc}(1 + y_s + y_p)[\Omega m^{-1}] \quad (3)$$

Where R_{dc} refers to the resistance of the conductor in direct current while y_s and y_p to the refers to the skin effect factor and proximity effect factor respectively [20]. The resistance of the conductor in direct current depends on the operating temperature T , resistivity ρ_{20} measured at $T_0=20^\circ\text{C}$, α_{20} the temperature coefficient at 20°C and cross section of the conductor S .

$$R_{dc} = \frac{\rho_{20}}{S} [1 + \alpha_{20}(T - T_0)] \quad (4)$$

The skin factor is calculated as

$$y_s = \frac{x_s^4}{192 + 0.8x_s^4} \quad (5)$$

where,

$$x_s^4 = \left(\frac{8\pi f K_s}{R_{dc} 10^7} \right)^2 \quad (6)$$

$K_s = 1$ in the case of a solid round conductor. As the transmission lines are three phased cables, proximity factor is calculated as,

$$y_p = \frac{x_p^4}{192 + 0.8x_p^4} (d_c/s)^2 [0.312(d_c/s)^2 + \frac{1.18}{\frac{x_p^4}{(192+0.8x_p^4)} + 0.27}] \quad (7)$$

where d_c is the conductor diameter and s is the the distance between conductors' axes, when the three conductors are equally spaced [20], $K_p = 1$ for copper round solid or stranded conductors, $K_p = 0.8$ for tubular round conductors and,

$$x_p^4 = \left(\frac{8\pi f K_p}{R_{dc} 10^7} \right)^2 \quad (8)$$

2.3.2 Reactance

The series reactance X_{k-m} is of inductive nature, calculated by:

$$X_{k-m} = 2\pi fL * l_{k-m} \quad (9)$$

Where, the frequency in the infield system in 50Hz , L is the inductance per unit of length given by the manufacturer and l_{k-m} the length of the section.

2.3.3 Shunt Capacitance

For the shunt elements of the model, the G_{k-m} is considered negligible. Whilst the shunt capacitance is defined as $Y_{shunt} = jB_{k-m}$ is calculated as:

$$\frac{Y_{k-m}^{sh}}{2} = j\pi fC * l_{k-m} \quad (10)$$

here, the frequency in the infield system in 50Hz , C is the capacitance per unit of length given by the manufacturer and l_{k-m} the length of the section.

2.3.4 Ybus matrix

Y_{bus} is defined as the bus admittance matrix, it is a symmetric matrix. Where Y_{ii} , the self-admittance, is equal to the sum of the primitive admittances of all the components connected to the i th node. And, Y_{ij} is equal to the negative of the primitive admittance of all components connected between nodes i and j . The admittances are calculated using the π -model and equations (1-10).

2.4 Power flow analysis

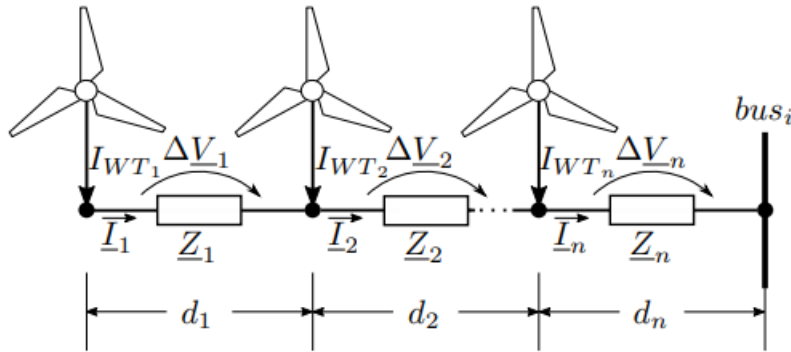


Figure 6: Single-line diagram of one feeder string [21]

The grid is modelled as shown in figure 6, treated as a transmission grid with generator buses and a load bus. With the Z element includes the π -scheme presented before. Each wind turbine injects I_w to the grid and the substation bus acts as slack bus providing the reference voltage and angle. The study will restrict the attention to a three-phased balance system steady operation. Where the power flow equations are as follows [22]:

$$P_i = \sum_{k=1}^n |V_i||V_k|[G_{ik}\cos(\theta_i - \theta_k) + B_{ik}\sin(\theta_i - \theta_k)] \quad i = 1, 2, 3, \dots, n \quad (11)$$

$$Q_i = \sum_{k=1}^n |V_i||V_k|[G_{ik}\sin(\theta_i - \theta_k) + B_{ik}\cos(\theta_i - \theta_k)] \quad i = 1, 2, 3, \dots, n \quad (12)$$

Where G_{ik} are called conductances and the B_{ik} are called susceptances and θ_i is defined as the angle of V_i . To solve such equations the procedure of [22] with Newton-Raphson method is used. Where, the equations involving P_1 and Q_1 are stripped away [22]. Remaining to find the n-1 unknown of $|V_i|$ and n-1 unknown of θ_i . As such vectors are defined and a composite vector x also.

$$\boldsymbol{\theta} = \begin{bmatrix} \theta_2 \\ \theta_3 \\ \vdots \\ \theta_n \end{bmatrix} \quad |\mathbf{V}| = \begin{bmatrix} |V_2| \\ |V_3| \\ \vdots \\ |V_n| \end{bmatrix} \quad \mathbf{x} = \begin{bmatrix} \boldsymbol{\theta} \\ |\mathbf{V}| \end{bmatrix} \quad (13)$$

Similarly the equation $\mathbf{f}(\mathbf{x})$ corresponds to:

$$\mathbf{f}(\mathbf{x}) = \begin{bmatrix} P(\mathbf{x}) \\ Q(\mathbf{x}) \end{bmatrix} \quad (14)$$

Setting the equations in the form $\mathbf{f}(\mathbf{x})=0$ becomes:

$$\mathbf{f}(\mathbf{x}) = \begin{bmatrix} P_2(\mathbf{x}) - P_2 \\ \vdots \\ P_n(\mathbf{x}) - P_n \\ Q_2(\mathbf{x}) - Q_2 \\ \vdots \\ Q_n(\mathbf{x}) - Q_n \end{bmatrix} = 0 \quad (15)$$

Each partition of the matrix \mathbf{J} is $(n-1) \times (n-1)$ p With \mathbf{J} , the Jacobian matrix \mathbf{f} considered as :

$$\mathbf{J} = \begin{bmatrix} \mathbf{J}_{11} & \mathbf{J}_{12} \\ \mathbf{J}_{21} & \mathbf{J}_{22} \end{bmatrix} \quad (16)$$

such that equation 17 becomes 18 after partitioning $\mathbf{f}(\mathbf{x})$:

$$\mathbf{J}^v \Delta \mathbf{x}^v = -\mathbf{f}(\mathbf{x}^v) \quad (17)$$

$$\begin{bmatrix} \mathbf{J}_{11}^v & \mathbf{J}_{12}^v \\ \mathbf{J}_{21}^v & \mathbf{J}_{22}^v \end{bmatrix} \begin{bmatrix} \Delta \boldsymbol{\theta}^v \\ \Delta |\mathbf{V}|^v \end{bmatrix} = \begin{bmatrix} \Delta \mathbf{P}(\mathbf{x}^v) \\ \Delta \mathbf{Q}(\mathbf{x}^v) \end{bmatrix} \quad (18)$$

2.4.1 Per unit system

When many transformers and voltage levels are involved, it is convenient to normalize the variables. In power system, per unit normalization is nearly almost chosen. Where the general definition stands as:

$$\text{quantity in per unit} = \frac{\text{actual quantity}}{\text{base value of quantity}} \quad (19)$$

Advantages of this utilization include: elimination of transformers in the per phase diagram, constants are more uniform making it possible to spot obvious data errors and the number in the result is more easily interpreted physically. In the case of this thesis, per unit normalization allows to evaluate directly the voltage drop in percentage from one turbine to the substation.

The procedure is summarized as follows[23]:

1. Pick a volt-ampere base for the whole system. In this work the volt-ampere base is the rated power of one turbine.
2. Pick one base voltage arbitrarily. Where in this work, this voltage is the infield grid medium level voltage of 33kV.
3. Find the impedance's bases as:

$$S_B = V_B I_B \quad V_B = Z_B I_B \quad Y_B = \frac{1}{Z_B} \quad (20)$$

4. Solve for desired per unit quantities, such as the voltage in each turbine node and current in each cable section.
5. Convert back to actual quantities if desired.

2.5 Cost Models

The cost to be optimized is related to two branches, the cost related to the installation of the cable and the cost derived from energy loss.

2.5.1 Cable Cost

The cost of installation of the cabling of the OWPP infield accounts to the capital investment (CAPEX) of the installation of the OWPP. Where studies such as [24] compare three different cost equations. Where the first is a cost formula for medium voltage such that:

$$C_c = K_1 + K_2 \exp(K_3 * I_n / 10^5) [k\text{€}/km] \quad (21)$$

Where I_n represents the cable ampacity in [A] and K_1 , K_2 and K_3 are coefficients depending on nominal voltage level. Whose value for 30-36 kV are $K_1 = 52.08$ [k€/km], $K_2 = 75.51$ [k€/km] and $K_3 = 234.34$ [1/A]. In addition it also reports data on average cost by authors' investigation on available cables. Formulating with least-square linear regression the following function in base of the cross section S [mm²]:

$$C_c = 0.4818S + 99.153 [k\text{€}/km] \quad (22)$$

The cable distance in this work will be considered the Euclidean distance between the coordinate points of wind turbine and wind turbine or wind turbine and substation. The total investment cost of the infield collection system is the sum of individual sections.

$$TC_c = \sum_{i=1}^{n_{sec}} l_i * C_c^i [k \text{€}] \quad (23)$$

For this study the individual cost of each cable will be used by equation 22 for the multi-objective function with in each infield collection. In addition, as the study also evaluated different collection system diagrams, the cost of transport, installation are taken into account where average cost from authors' investigation on cable laying services is reported in table 3. This is indifferent of the cable diameter so is only calculated with the total cabling distance of each layout. Other CAPEX components such as wind turbines, transformers or other electrical equipment are equal for all designs and so are not considered in the optimization.

Table 3: Cable transport and installation cost data [k€/km] [24]

	Cost
Transport	72
Intalation	391

2.5.2 Energy Loss Cost

The loss of energy in cables and thus energy not sold to the grid is considered as an energy cost. This fictional cost is an operational expenditure (OPEX) is calculated yearly by the power loss and full load hours (FLH) of the OWPP.

$$E_{loss} = P_{loss} * FLH \quad (24)$$

In order to compare the CAPEX cost with an OPEX cost, the working time if the OWPP needs to be taken into account, the discount rate and energy cost to obtain the net present value (NPV) of the energy cost. Which will be taken as shown in table 4.

$$NPV = E_{loss} * C_{electricity} * \sum_{t=1}^{years_{life}} (1 + r)^{-1} \quad (25)$$

The levelized cost of energy (LCoE) is considered as energy cost as it is the minimum electricity price to break even. For this study the lower bound of the LCoE is taken as predictions for offshore wind energy reduce the LCoE in following years. For the FLH a midpoint of 3850 will be used. The share of debt and equity can be explicitly included in the analysis by the weighted average cost of capital (WACC) over the discount factor[25].

Table 4: Economic Parameters based on [25]

$WACC_{real}$	LCoE	Full load hours	Lifetime
5.24%	7.23 €cent/kWh and 12.13 €cent/kWh.	3200-4500	25 years

2.6 Graph theory

Graph theory is a branch of mathematics which is concerned on the analysis of networks of points connected by lines. These points and lines are referred to as edges and vertices. Unless otherwise stated, the style simple graph is assumed. [26] But, different arrangements of vertices and nodes create different styles of graphs as shown in figure 7. Yet, there are two main denominations for a graph. A directed graph, where you can denote the flow and cost of each edge. Whereas, an undirected graph, one can set only the cost or weight of an edge. For the creation of all the possible edges to be used in this thesis it is important to get as close as possible to a complete graph. However, this increases the computational power needed and time to solve the path problem. In addition, it is more important to avoid the creation of a multigraph or a loop in the graph.

An important number associated to avoiding the previous two styles is the vertex degree. Which is defined as the number of edges that enter or exit from it [26]. In this manner, a loop would be associated to increasing the vertex degree by two.

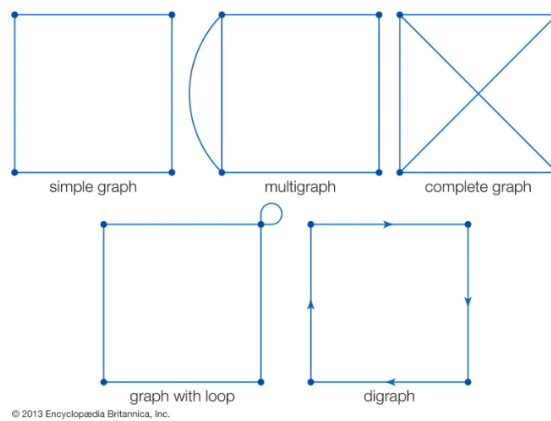


Figure 7: Basic type of graphs [26]

2.7 Optimization model

Each possible combination of cables creates a set of cable installation cost and energy loss cost. Where there is a trade off between cost. This creates the need to set it as a Multi-Objective Combinatorial Optimization Problem (MOCOP). Which is defined by [27] as:

$$(MOP) = \begin{cases} \text{Optimize} & F(x) = (f_1(x), f_2(x), \dots, f_n(x)) \\ \text{with} & x \in D \end{cases}$$

where n is the number of objectives ($n \geq 2$), x is the decision variable vector and D is the set of feasible solutions and $f_i(x)$ to be optimized. The solution of a MOCOP is not unique, it is composed to a set of solutions representing the best trade-offs amongst the objectives. These solutions are contained in the Pareto optimal set (PO) when plotted the Pareto front of the problem is obtained. Such as shown in figure 8:

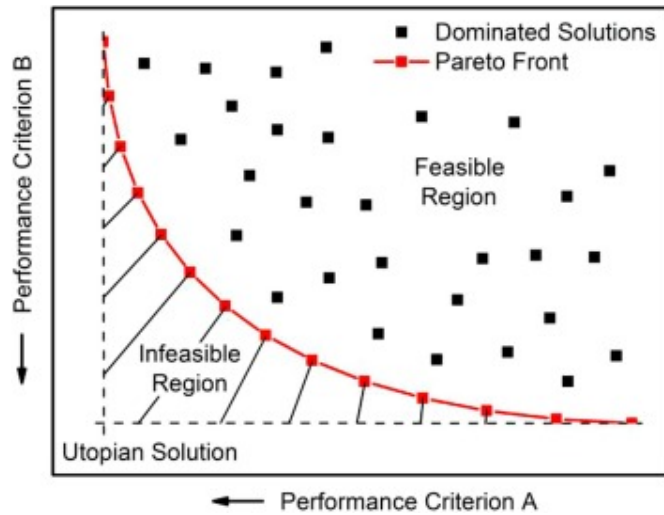


Figure 8: Pareto Front [28]

To obtain the PO of the solution set, dominance has to be established between the feasible solutions $x \in D$. Such that $x^* \in D$ is denoted Pareto optimal, if and only if there is no other solution that dominates over it.

A solution $\mathbf{a} = (a_1, a_2, \dots, a_n)$ dominates over solution $\mathbf{b} = (b_1, b_2, \dots, b_n)$ if two criteria are met.

$$if \begin{cases} \forall i \in [1, 2, \dots, n] & f_i(\mathbf{a}) \leq f_i(\mathbf{b}) \\ \exists i \in [1, 2, \dots, n] & f_i(\mathbf{a}) < f_i(\mathbf{b}) \end{cases}$$

Any solution of the PO may be considered as optimal, due to the fact that no improvement may be found for an objective without degrading another objective value[27]. In this method, some terms are useful to be noted to make a decision[29].

(a) Anchor point : Obtained through the best of each objective function. Or in other words treating each $f_i(x)$ as a single objective function.

(b) Utopia point: In a two function problem. It is defined as the intersection of the anchor point value of the function $f_1(x)$ and the anchor point value of function $f_2(x)$.

Comparing the values of x^* with in each other depends on the weight that the decision maker sets for each objective function. However, in a MOCOP with no clear function weights the optimal solution can defined as the x^* with the shortest Euclidean distance to the Utopia point[29]

3 Design tool description

In this chapter, the DT is presented. Starting by the distribution of the program, the inputs necessary to run and the explication of algorithms. The DT has the objective of determining the optimal design of the electrical configuration of an OWPP. It is assumed the location of the wind turbines and substation has been predetermined by previous analysis. Such that the DT has to determine the layout and cable diameters to be set. The theory presented in Chapter 2 is utilized to plan the decision making in six main steps as shown in table 5 .

Table 5: Sections of the DT

Section of DT	Inputs needed from User
1. Generate a graph model of the OWPP	Cordinate system of WT location standardized in 1/D Location of substation Rotor diameter (D)
2. Create the possible cable connections.	Maximum distance allowed to cable between turbines Maximum distance allowed to cable between any turbines and the substation Number of possible connections to the substation
3. Find shortest total cable distance of the combination of cable connections to connect all wind turbines.	Number of connections to substation Number of WT connected to each string
4. Find the value of cost of cabling and energy cost for the different combination of cable diameters.	Cable information Economic parameters Power and voltage base
5. Optimize point 4 results with the Pareto front.	
6. Present a summary of elements on the final result.	

3.1 Algorithms

The six previous steps can be grouped into two main algorithms. The first is the one in charge of obtaining the cable layout. To start it loads up all user inputs including two csv files. Beginning with the set of coordinates for the turbine location, and the secondly a table containing the information of the cable possibilities. All other inputs are currently set in the beginning of the code. The code utilizes pre-set functions from Matlab graph selection to create the graph object, edges and obtain the sets of paths. The sets are then transformed to Boolean arrays, where a 1 means that the edge or node is present in the set, whilst a zero means it is not present in such set. These arrays are combined in a loop until an array of all all nodes being present is found

saving the resulting vector combination of edges. It is important to note that the line intersection detection is aided by [30] code where it finds the coordinate of the intersection of two lines, this intersection is evaluated if it is in the range created by the nodes. Finally all combinations are arranged by total Euclidean distance, thus the optimal distribution ends in the top row of the matrix. This algorithm is in figure 9.

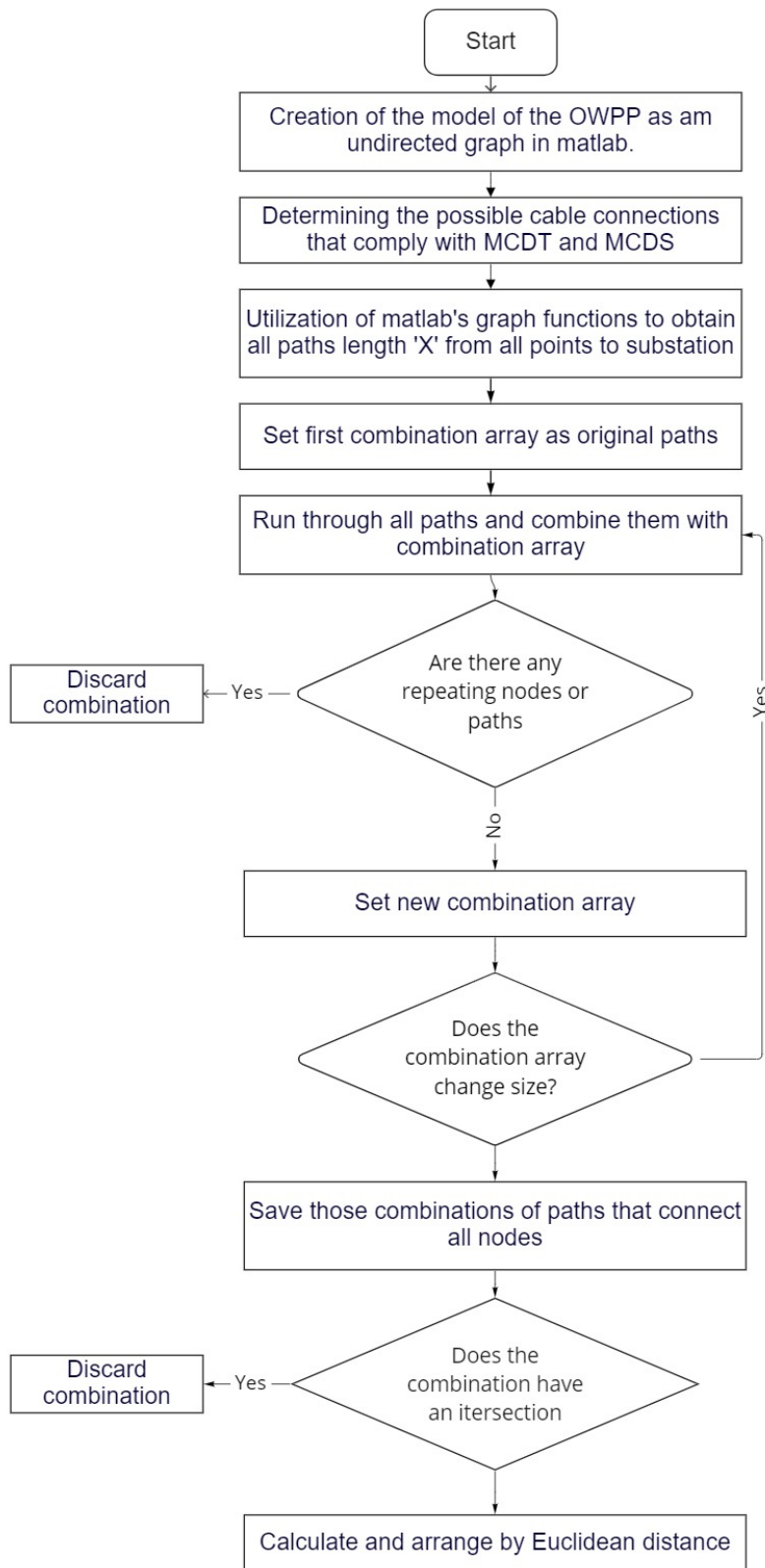
The second section of the DT defines the diameter of each cable by a multi-objective function comparing the cable cost and the energy loss cost. It begins by loading the viable array of edges from the previous section. Utilizing the user input of string length and possible cross section of cables to be used, it uses an indexing vector to generate all possible arrangements of cable cross sections with in a string. For every arrangement it calculates the cable cost according to the euclidean distance between nodes and equation 22. Additionally, it uses NR to calculate the voltage of each node and current in each cable section using equations [1-18]. The voltage and current limitations are checked and those iterations that pass the power loss is transformed into energy loss with equations [24-25]. The viable results are compared with each other, obtaining the dominant set and thus the Pareto front, anchor points and utopia point. Finalizing with calculating all euclidean distances from the utopia point to the points in the Pareto front and identifying the shortest one as the optimal solution. This algorithm is shown in figure 10.

3.2 Limitations

As stated beforehand, the DT was created with two objectives. The first one is to dictate the best cable configuration based on a set of possible edges, and the second one is an optimization of cable diameter to limit the effect of cable cost and energy loss cost. However, it has to be noted that the tool does pose certain limitations that may hinder the overall result.

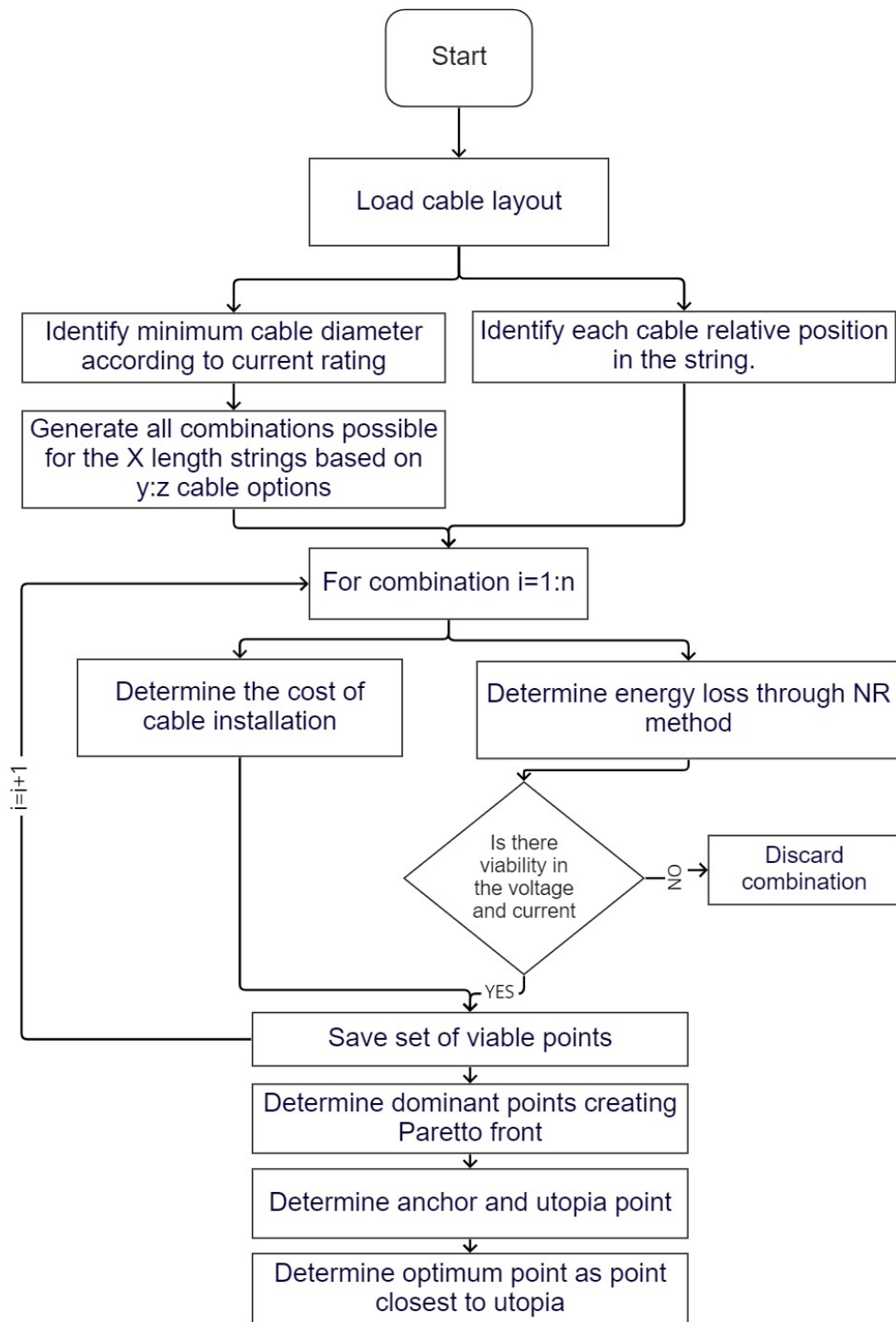
The first limitation presented is the position of the substation, this analysis does not evaluate where such substation should be placed. This decision is completely arbitrary by the user or should be done with previous analysis. For example, using fuzzy C-means clustering as investigated in [31] which divides the OWPP into sub areas.

Secondly, the limitation of computer power and time restricts in two main areas. To start with is the possibility of evaluating edges in the graph. The tool limits the distance of such edges as an increase in possible edges increases exponentially the time to combine them. Furthermore, the DT is built so that it only allows strings of equal size to be connected, limiting the OWPP topology options. In addition, when evaluating the different diameters of each section, these are evaluated depending on the order they have in the string, not as individuals for the same reason. This could be troublesome in distributions where two different strings have different distance distributions.



miro

Figure 9: Algorithm to calculate the total distance of all viable cable layouts



miro

Figure 10: Algorithm for cable diameter decision

4 Case Study

In this chapter the DT is used in a specific OWPP distribution. Where, the parameters chosen are presented and the results are discussed at the end of the chapter.

4.1 Input Data

As presented before in table 5, certain parameters need to be set by the user.

Table 6: Inputs considered for case study

Variable	Value
Rated Voltage	33 kV
Wind turbine model	SWT-7.0-154 [32]
Rated power	7 000 kW
Power Factor	1
Rotor Diameter (D)	154 m
Number of wind turbines	24
Topology	4 x 6
Horizontal Spacing	9D
Vertical Spacing	7D
Maximum cable distance between turbines (MCDT)	10D
Maximum cable distance between turbines and substation (MCDS)	10D
Connections to substation	4
Substation location	(13 D ; 26,25 D)
Cable information	shown in Table 2

4.1.1 Farm layout

Knowing the topology, horizontal and vertical spacing, the substation location, MCDT and MCDS the DT creates a graph such as figure 11 with all the possible edges represented in blue and nodes represented in black to be evaluated.

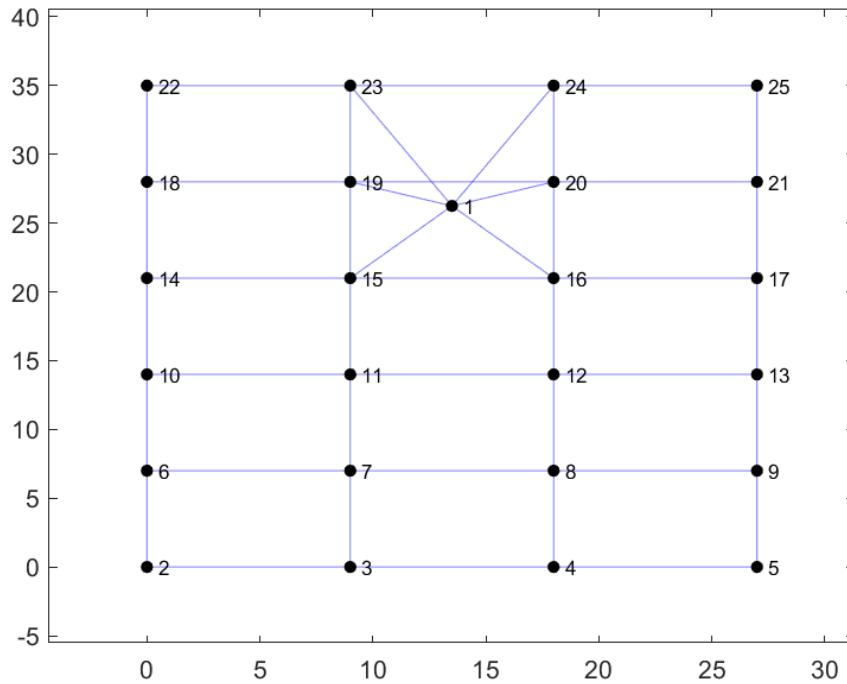


Figure 11: OWWP layout represented in a graph

4.2 Layout distribution

For the possible connections showed in figure 11 the DT found a total of 482 different paths to connect six turbines to the substation. Afterwards combining them to find 17 different distributions that connect all turbines to the substation, non of which had any cable crossing. The one with minimal total distance is shown in 12 with a value of 26 409 m.

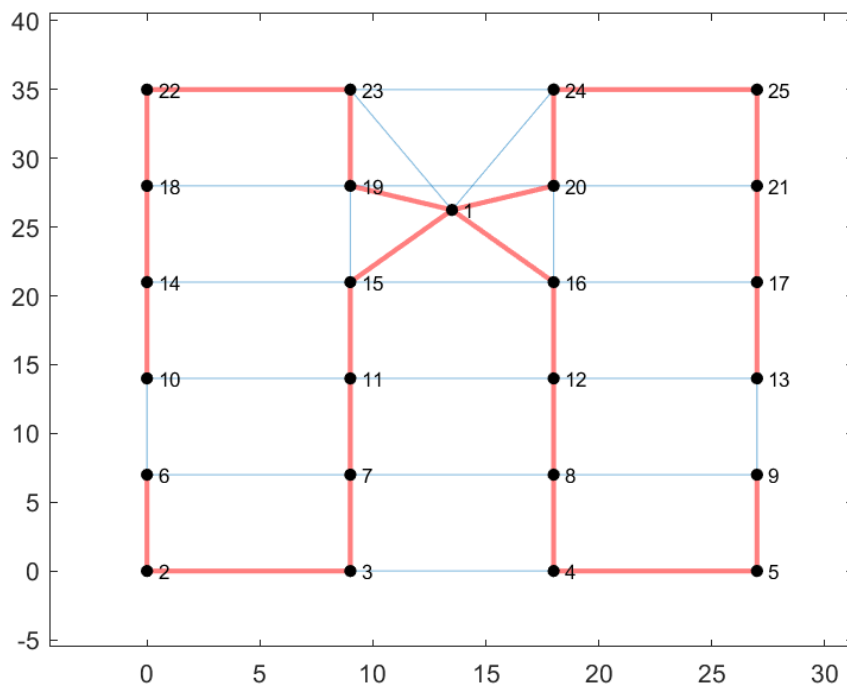


Figure 12: Least distance set up for cable distribution

In figure 13 the subsequent distributions are shown with total distance of 26 717 m and 26 859 m.

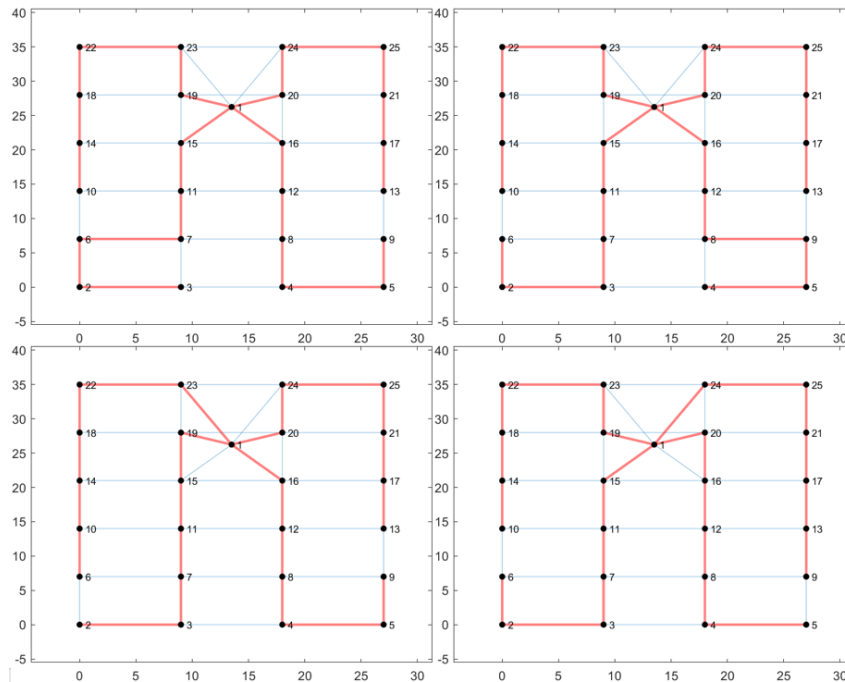


Figure 13: Subsequent layout distributions

4.3 Combination of cable diameters

To calculate the cable diameter parameters the DT found the minimum cable for each section. It is important to note, that section 1 is defined as the one connected to the substation whilst section 6 the one connecting the last turbine in the string.

Table 7: Minimum cable per section position

Section position	Minimum Cable number	Maximum current foreseen (A)	Cable current Capacity (A)
1	10	734,81	775
2	8	612,34	655
3	6	489,87	530
4	3	367,40	375
5	1	244,94	300
6	1	122,47	300

As shown in table 7 the DT takes that combination as the initial test, and a combination of all diameters equal to the largest possible cable. In this particular case it generates 12 000 cable combinations to test, from which the result of cable cost vs energy loss cost relationship is shown in figure 14 in Euros.

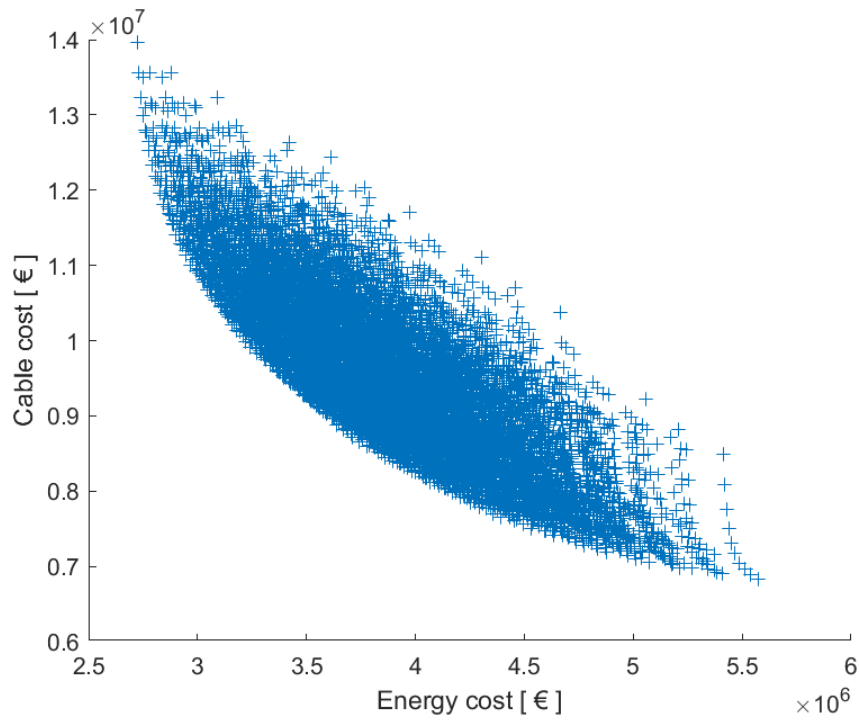


Figure 14: Combination distribution on a comparison of Energy loss cost and cable installation cost

From the previous figure, the dominance of the points is determined to obtain the Pareto front as a result. For this case study, there are 149 dominant points and are shown in 15.

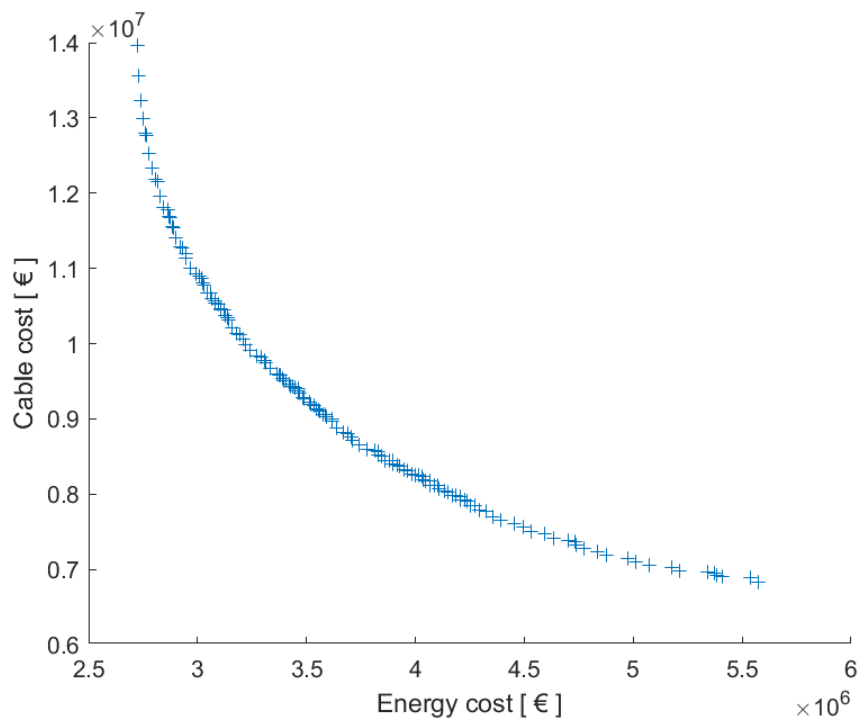


Figure 15: Pareto Front of combinations

Out of this 149 dominant points the two anchor points are identified, each as the best combination for each objective function. Additionally the utopia point is calculated with the combination of both. These are identified in table 8 and graphically seen in figure 16.

Table 8: Anchor and Utopia point

Point	Combination	Total Cost
Anchor 1	10 ; 10 ; 10 ; 10 ; 10 ; 10	16 691 879,12 €
Anchor 2	10 ; 8 ; 6 ; 3 ; 1 ; 1	12 412 755,46 €
Utopia Point	-	9 560 710,04 €

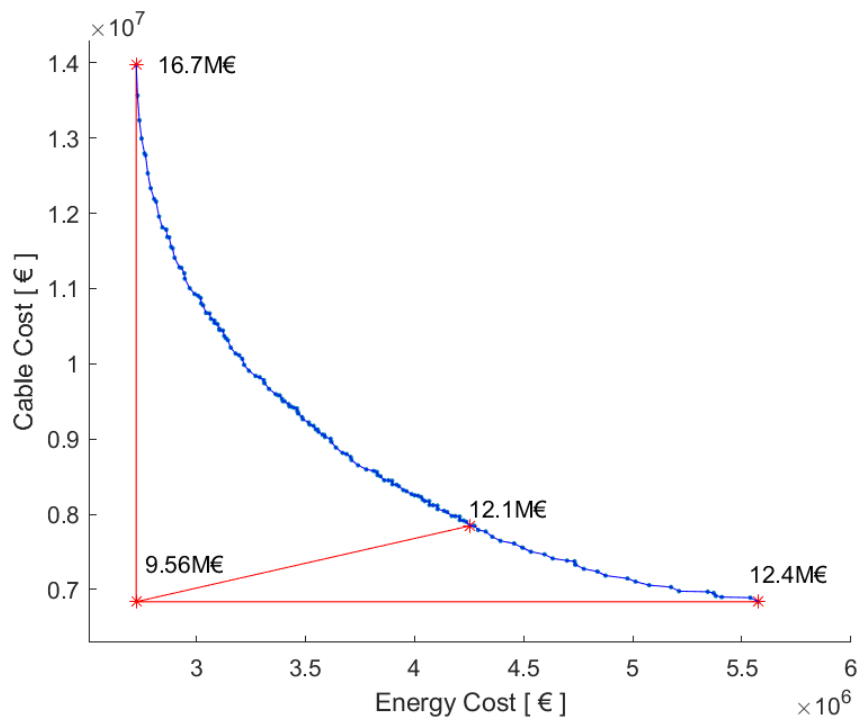


Figure 16: Pareto Front analysis

The optimal solution is found according to the shortest euclidean distance to the utopia point. This point contains the cable selection as: [10 8 7 6 5 2] for each string, with a total cost of 12 100 137,18 €. The distribution of the different cable diameters is graphically shown in figure 17.

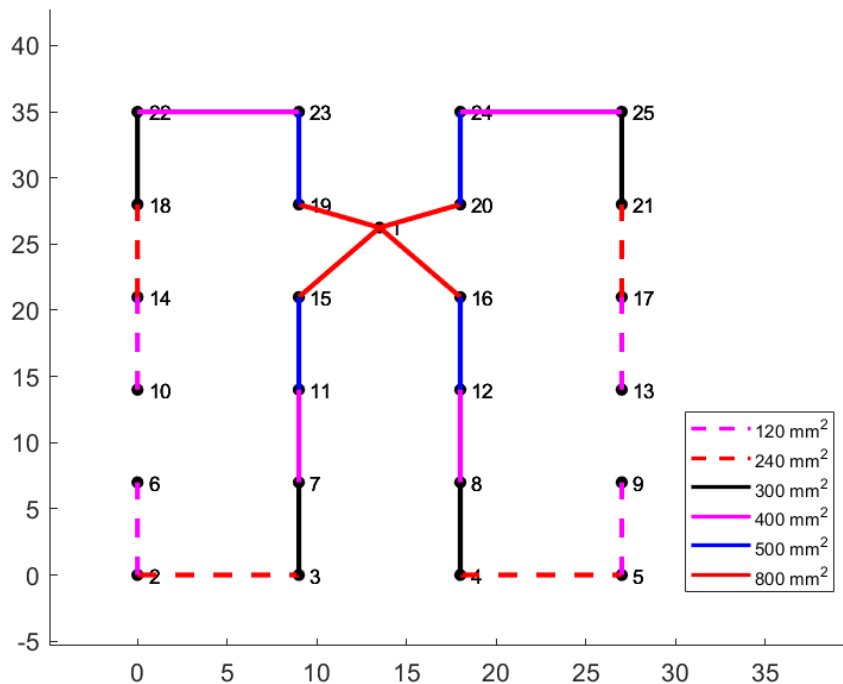


Figure 17: Cable diameter installment

4.4 Optimal distribution analysis

As mentioned before, this solution cost 12 M€ in total comparable cost. Which is divided into 4 254 529,82 € derived from energy loss over 25 years and 7 845 607,36 € derived from the cable cost. The energy loss cost is calculated from a power loss of 1055,41 W; which percentage wise is translated to 0,63% of the OWPP production in steady state. To set the energy loss into context, the anchor points in table 8 are also evaluated. The first anchor point, with the maximum cable diameter, the power loss is 0.40%. On the other hand, when evaluating anchor point number two, the power loss is 0,82% of the production.

When evaluating the anchor points in cost cable, the upper bound is found in anchor one with a cost value of 13,97 M € whilst the lower bound is in anchor two with a value of 6,84 M €. Focusing on figure 18 it can be noted that the data distribution of the cable cost is more spread out than the energy loss cost data. In addition, the optimal point chosen by the DT sets the cost of energy loss cost above the 3rd quartile line, whilst below the cable cost 1st quartile line.

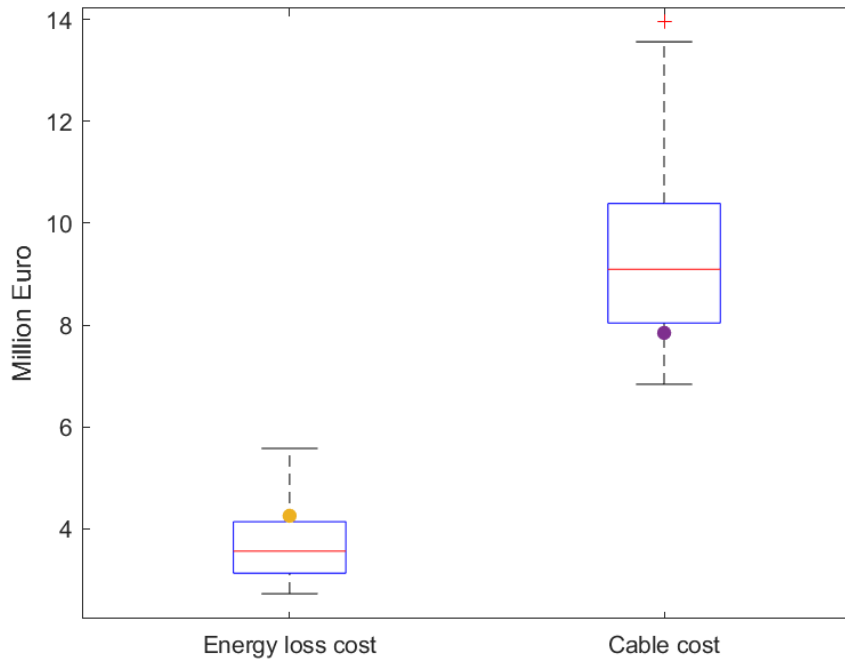


Figure 18: Box and whiskers plot representing the different Pareto front cost distribution

Lastly, when analyzing the voltage in each node. The optimal solution generates figure 19, where two things can be noted. First of all, the largest voltage is 1,1% larger than the substation voltage, being in the acceptable range for transmission systems. Secondly, since there are two different types of connection strings, the node voltage in the turbines near the substation vary.

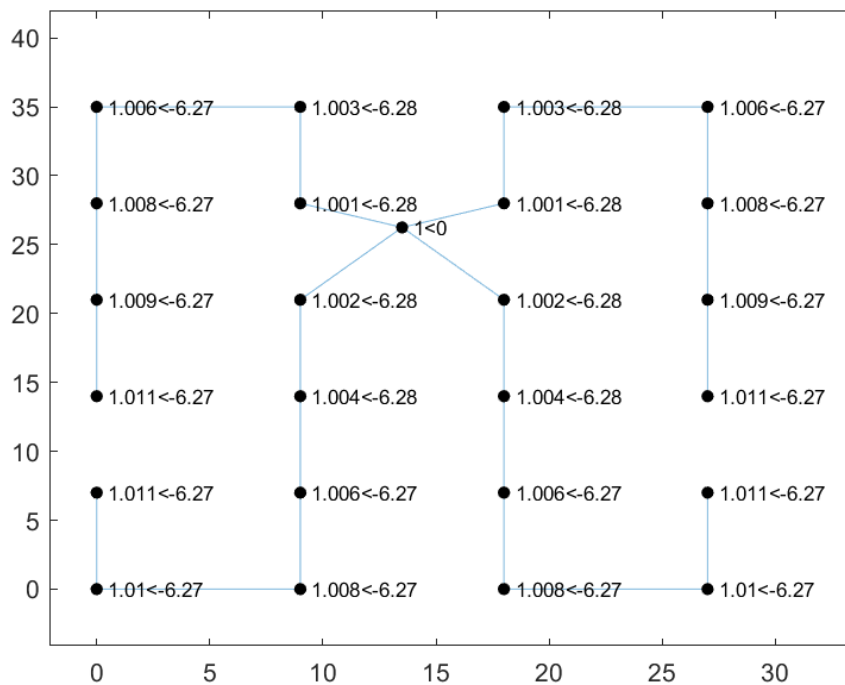


Figure 19: Node voltage in each turbine node.

5 Analysis of the performance of the design tool

In this chapter, two performance analysis are undertaken. First analysing the time performance of solving the case study. Secondly, a sensitivity analysis on the possible price change of the electricity price, resulting in a change of the Pareto optimum combination.

5.1 Performance of DT in solving case study

The DT was coded and ran using Matlab 2021b, where the case study computational times shown in table 9. It is notable that the mayor time management sections are the creation of the combination of layouts and the multi objective function results calculation.

Table 9: Time ditribution in running the DT

Section	Section time (s)	Total time (s)
"Generate a graph model of the OWPP"	1,86	1,86
"Create the possible cable connections."	0,1	1,95
"Find shortest total cable distance of the combination of cable connections to connect all wind turbines."	269,94	271,89
"Find the value of cost of cabling and energy cost for the different combination of cable diameters."	422,74	694,64
"Pareto Front"	0,77	695,41
"Result presentation"	1,37	696,77

As mentioned in 2.1 any DT created should aim to cover three main ideas. For this reason, the tool was tested with an increasing number of possible connections from the substation to different turbines. From this test; two figures were obtained. In figure 20 three variables are noted, starting with the number of singular strings found to connect six turbines with the substation. In this variable, a linear increase is perceived. Secondly, the number of possible viable combinations has a logarithmic tendency. This tendency has an increased detriment as an increase of combinations found that contain intersections also increases.

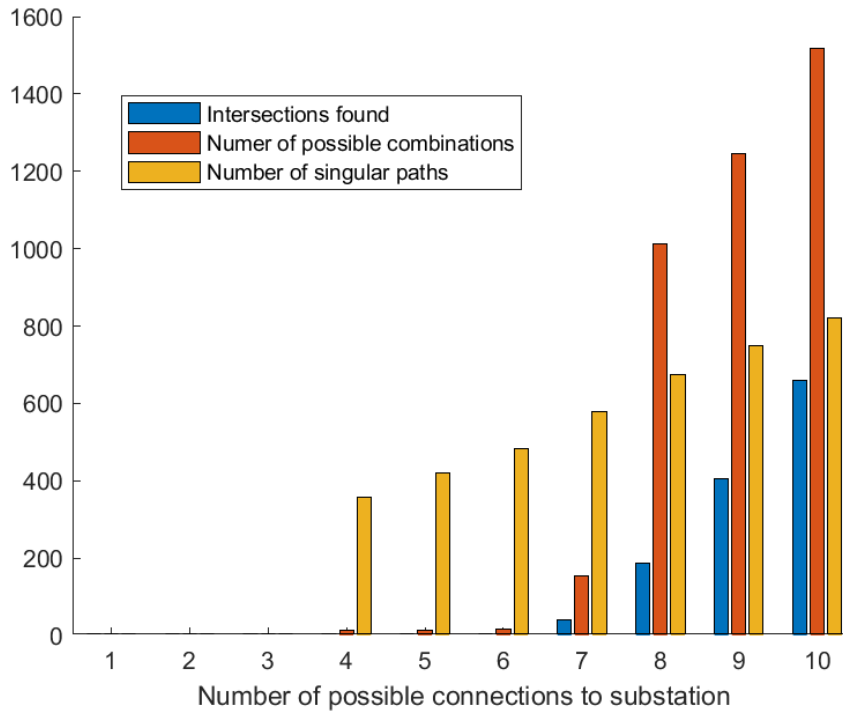


Figure 20: Number of results generated with increasing number of possible connections

With each increasing possible connection, the number of singular strings is increased as mentioned above. This entails an increase of computer power needed and thus the time to compute. As shown in figures 21 and 22 the increase in time becomes exponential, where further increase of time contradicts 2.1 a) objective.

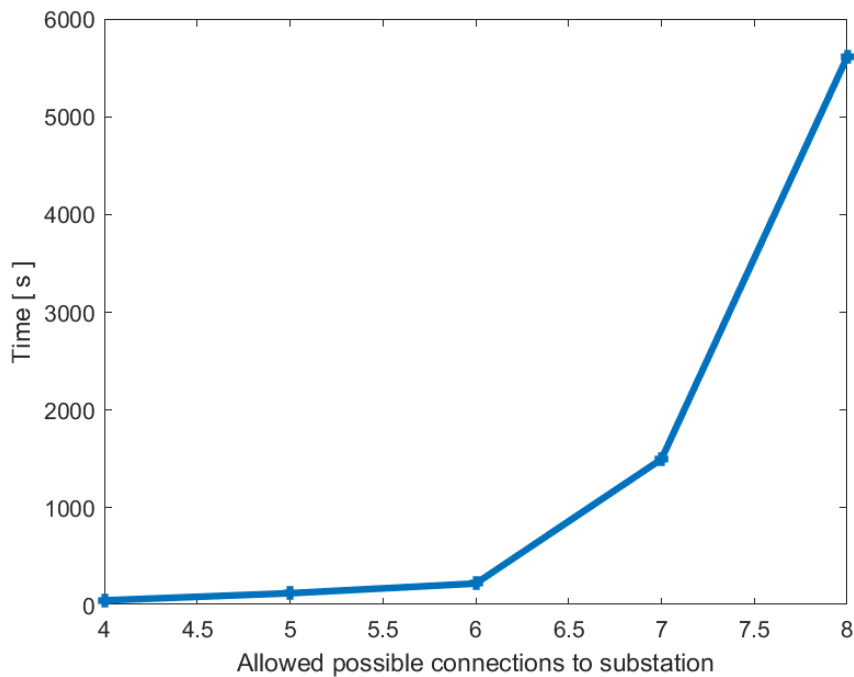


Figure 21: Time taken to undergo section 3 of the DT over increasing possible connections

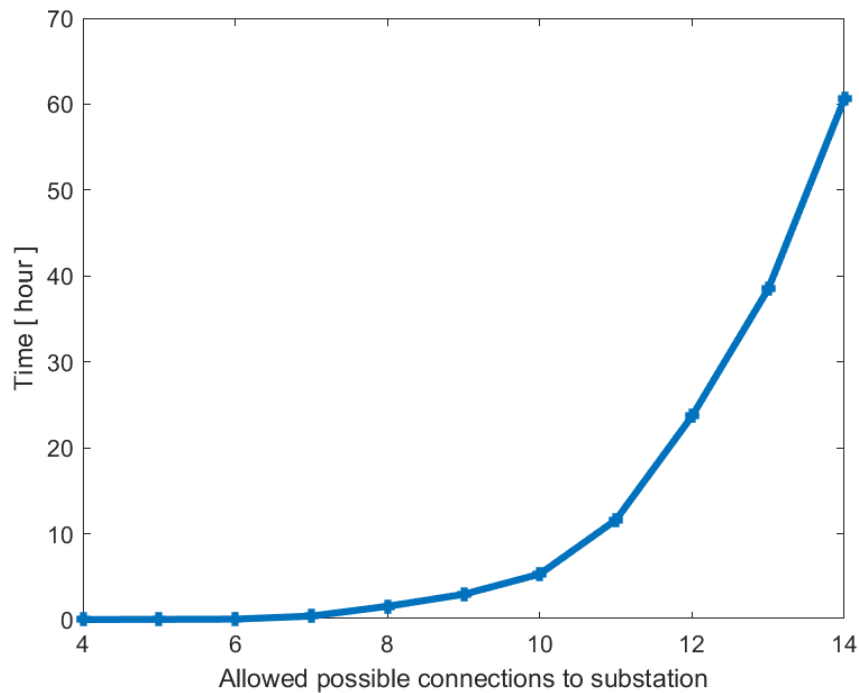


Figure 22: Time taken to undergo section 3 of the DT over increasing possible connections

5.2 Sensibility analysis

In this section, the fluctuation of energy price is taken into account by creating a sensibility analysis on what is the effect on the total cost with energy price fluctuations.

The analysis was done in ten points covering the LCoE range set in table 4. The resulting Pareto fronts are shown in figure 23, when increasing the LCoE in the simulation has two effects on such fronts. The most visible effect being a shift to the right in the graph. In addition, as the LCoE used in the simulation is increased there is a resulting horizontal widening of the Pareto fronts. This is more noticeable in the more inefficient cable combinations. The second effect on the Pareto front creates a change in the Pareto optimum point as shown in the red dots in figure 23. This results in a different optimum cable configuration that would be implemented in the project. It is important thus to note that when using the DT in a specific project it is important to evaluate the possible average LCoE of the 25 years the project will be operational.

When evaluating the different Pareto optimum points shown in red, it can be concluded that when utilizing an increasing LCoE the cable instalment cost also increases as shown in figure 24. It can then be thought that, with an increasing the cost of energy loss the DT designates a more efficient cable combination by increasing the diameter. Resulting in an increase in cable instalment cost.

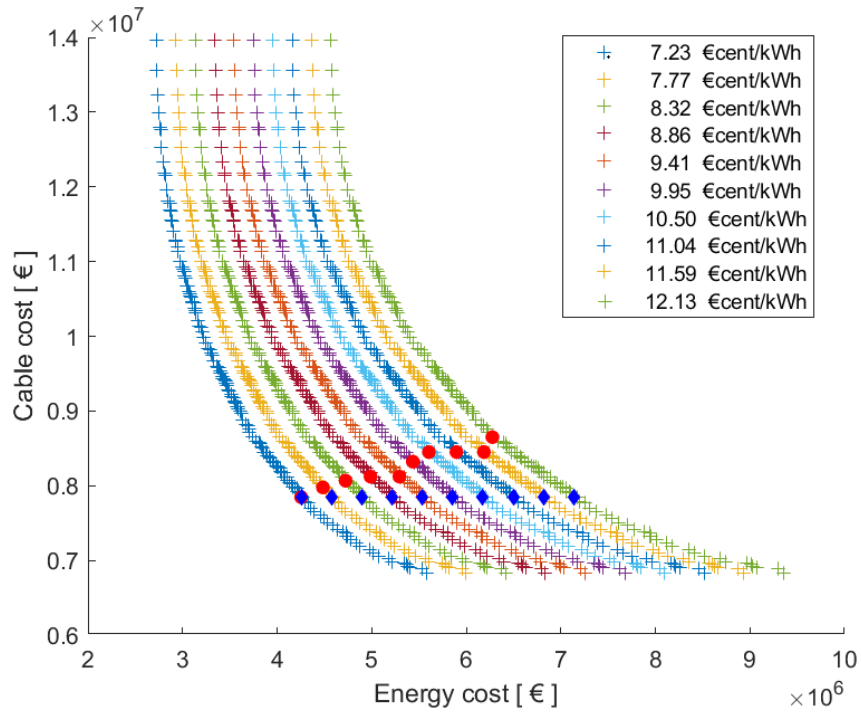


Figure 23: Box and whiskers plot representing the different Pareto front cost distribution

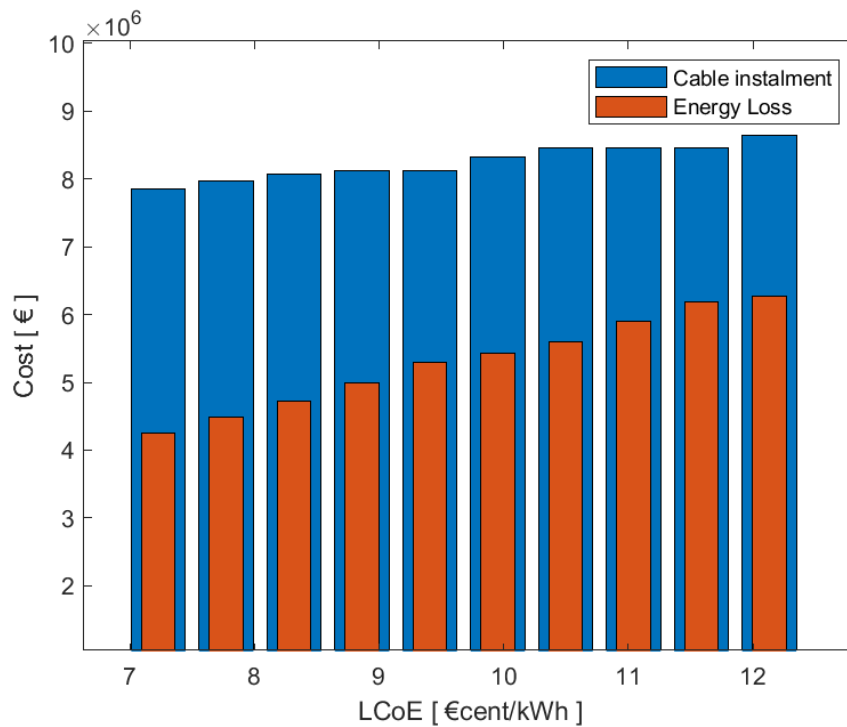


Figure 24: Comparison of shift in energy and cable related costs

It is interesting to note that even tho the cost of energy increases as the LCoE increases, when the values are standardized a different view is shown. Figures 25 and 26 illustrate the position

in percentile of the optimum data point with in the Pareto front range. Due to the fact the cable instalment range does not change an evident increase in percentile is shown in 25. On the other hand in figure 26 the opposite can be noted. The optimum point shifts to the left with in the Pareto front combinations and thus decreasing in the percentile. This can be due to the fact, as mentioned above, that the energy cost range increases also with an increasing LCoE.

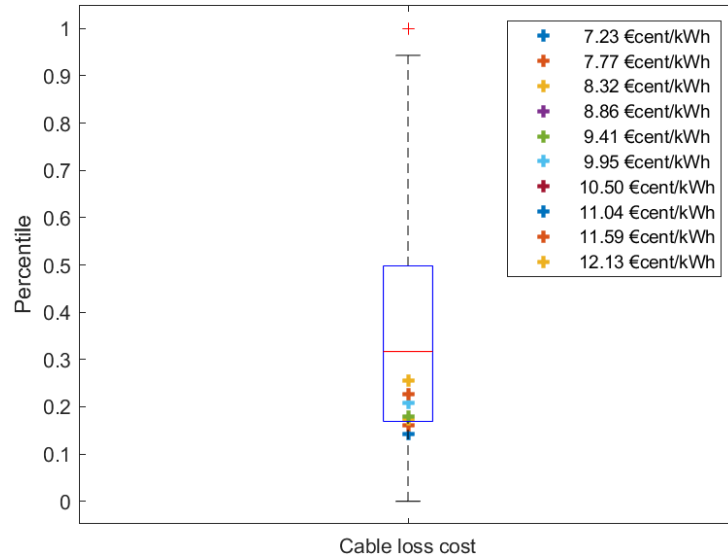


Figure 25: Box and whiskers plot with the iterations in change of LCoE used to simulate for cable related costs

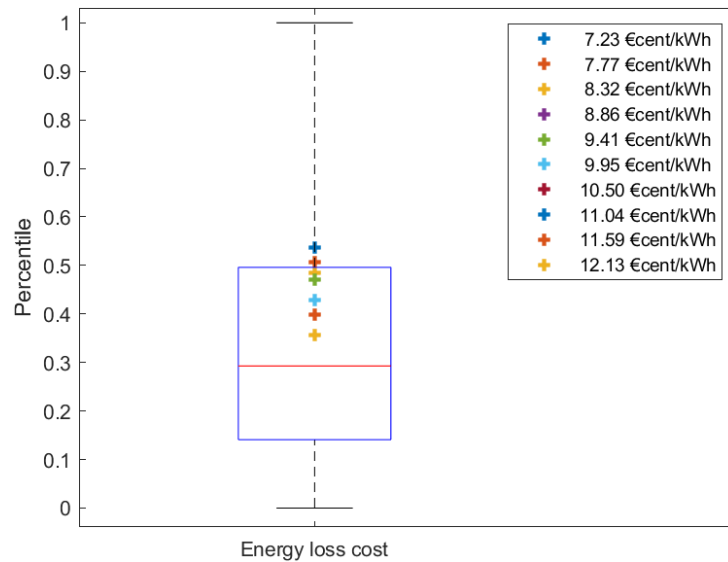


Figure 26: Box and whiskers plot with the iterations in change of LCoE used to simulate for energy related costs

A previous project to project base study of specific LCoE seems to be needed to choose the correct cable diameter distribution. However, with increase uncertainty in electricity prices one could not be sure the price will stay stable for the production and operation years of the OWPP.

In figure 23 the blue diamonds show then the position of the energy and cable cost if the optimal diameters would not be changed. In other words, the DT is simulated with the lowest LCoE to find the cable diameters, and then tested on how the energy loss cost changes whilst keeping the diameters the same in each iteration. When comparing its total cost with the ones from the Pareto optimum points (red dots) we can draw figure 27. Interestingly, it can be noted that the total cost of either are similar. With this in mind if a project is not sure on which LCoE to use, it is prudent to use the lowest one, supporting the assumption done for this work in 2.5.2.

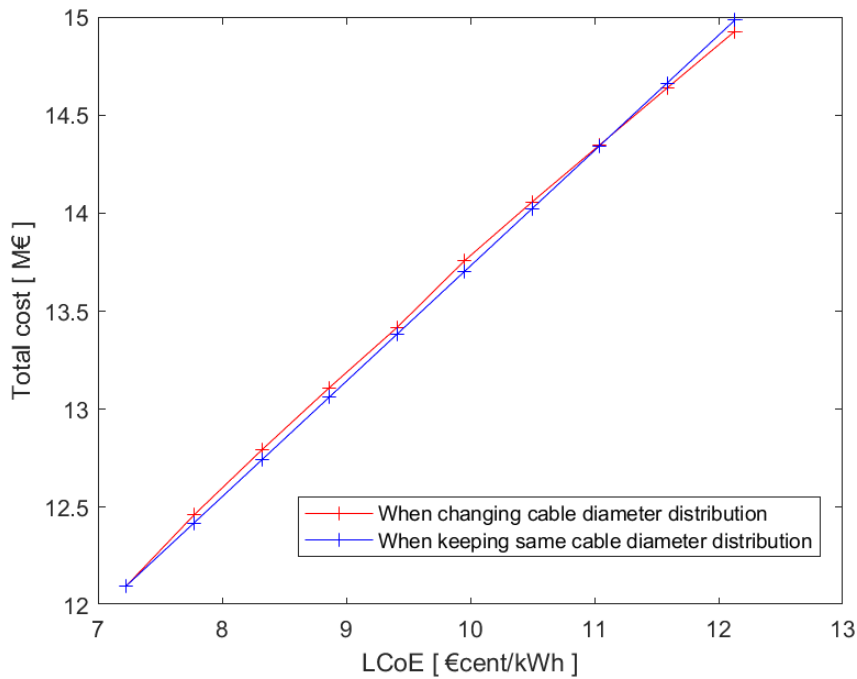


Figure 27: Total cost comparisons

Conclusion

This study took on the challenge of creating, testing and analyzing a DT to generate the inter-connection system of an OWPP. Such DT aims to optimize economically the cable layout and subsequently the cable diameter according to a multi objective function.

In an overview of the report, firstly a summary of previous research done on the subject is discussed. Where most works either focus on cable layout or cable diameter, and a few are shown to tackle both problems simultaneously. During the process of this study, the problem were tried to be tackled simultaneously with no avail. In the process of coding, it was decided to take on each problem one at a time. Resulting in a visible division of the algorithms as explained in chapter 3. This is followed by an explanation of theory on which the code was based on, such as graph theory, power flow theory, cost analysis and multi-objective functions.

The DT is tested in a case study based on 24 wind turbines connected to a substation. As mentioned before, the location of a substation is not part of this study, but as shown in the figures in appendix A different coordinates can be loaded into the program to calculate different layouts.

Consequently an analysis of the performance of the DT was undertaken, where the time utilized to run the different sections in the case study were recorded. Followed by a series of test on increasing the possible connections that the substation could have to turbines and its effect on the time consumption. Yet, as seen in appendix B the result does not change even if the time consumed is exponentially increased. Having in the specific circumstance of the case study a detrimental effect. Increasing the MCDT to include diagonals was also tried as shown in appendix C, however, the time to solve such graph was not realistic. As the program had to combine 57 536 individual strings.

The project achieves the goal of generating the optimal solution for the cabling of an OWPP. Yet, not without its limitations and possible future work. As stated before, the time constraint in this program is evident. An increase in possible connections or iterations on each cable separately could improve the result, for example in the case study, not all four strings have the same distance distribution. However, this increase in variables increases exponentially the computational time. Furthermore, a weighted circumstance between the functions of the multi-objective fiction could be applied with the desired of the client on the preference of energy loss or installation cost. As well as the limitation of a set of cables to be installed from the catalogue.

Bibliografia

- [1] Line Braendstrup. *Celebrating 30 years of offshore adventure*. 2021. URL: <https://www.siemensgamesa.com/en-int/explore/journal/2021/08/vindeby-30-anniversary-offshore>.
- [2] Wind Europe. *Our energy, our future How offshore wind will help Europe go carbon-neutral*. Tech. rep. Wind Europe, 2019.
- [3] Bureau of Ocean Energy Management. *Renewable Energy on the Outer Continental Shelf*. URL: <https://www.boem.gov/renewable-energy/renewable-energy-program-overview>.
- [4] Peng Hou et al. "A review of offshore wind farm layout optimization and electrical system design methods". In: *Journal of Modern Power Systems and Clean Energy* 7.5 (2019), pp. 975–986. DOI: [10.1007/s40565-019-0550-5](https://doi.org/10.1007/s40565-019-0550-5).
- [5] UK Department for Business Innovation Skills. *Review of Cabling Techniques and Environmental Effects Applicable to the Offshore Wind Farm Industry*. Tech. rep. Centre for Environment Fisheries and Aquaculture Science, 2008.
- [6] Manuel U.T. Rentschler, Frank Adam, and Paulo Chainho. "Design optimization of dynamic inter-array cable systems for floating offshore wind turbines". In: *Renewable and Sustainable Energy Reviews* 111 (2019), pp. 622–635. ISSN: 1364-0321. DOI: <https://doi.org/10.1016/j.rser.2019.05.024>. URL: <https://www.sciencedirect.com/science/article/pii/S1364032119303375>.
- [7] Sudipta Dutta and Thomas J. Overbye. "Optimal Wind Farm Collector System Topology Design Considering Total Trenching Length". In: *IEEE Transactions on Sustainable Energy* 3.3 (2012), pp. 339–348. DOI: [10.1109/TSTE.2012.2185817](https://doi.org/10.1109/TSTE.2012.2185817).
- [8] Constantin Berzan. "Algorithms for Cable Network Design on Large-scale Wind Farms". In: 2011.
- [9] Yunus Eroğlu and Serap Ulusam Seçkiner. "Design of wind farm layout using ant colony algorithm". In: *Renewable Energy* 44 (2012), pp. 53–62. ISSN: 0960-1481. DOI: <https://doi.org/10.1016/j.renene.2011.12.013>. URL: <https://www.sciencedirect.com/science/article/pii/S096014811100694X>.
- [10] Yuanhang Qi et al. "Simultaneous Optimisation of Cable Connection Schemes and Capacity for Offshore Wind Farms via a Modified Bat Algorithm". In: *Applied Sciences* 9 (Jan. 2019), p. 265. DOI: [10.3390/app9020265](https://doi.org/10.3390/app9020265).
- [11] Shurong Wei et al. "Hierarchical Optimization for the Double-Sided Ring Structure of the Collector System Planning of Large Offshore Wind Farms". In: *IEEE Transactions on Sustainable Energy* 8.3 (2017), pp. 1029–1039. DOI: [10.1109/TSTE.2016.2646061](https://doi.org/10.1109/TSTE.2016.2646061).
- [12] Peng Hou et al. "Overall Optimization for Offshore Wind Farm Electrical System". In: *Wind Energy* 20 (Dec. 2016). DOI: [10.1002/we.2077](https://doi.org/10.1002/we.2077).
- [13] Manuel U.T. Rentschler, Frank Adam, and Paulo Chainho. "Design optimization of dynamic inter-array cable systems for floating offshore wind turbines". In: *Renewable and Sustainable Energy Reviews* 111 (2019), pp. 622–635. ISSN: 1364-0321. DOI: <https://doi.org/10.1016/j.rser.2019.05.024>. URL: <https://www.sciencedirect.com/science/article/pii/S1364032119303375>.
- [14] Christoph Kaufmann. *Optimization of cable sizes of an offshore wind farm collector system using a multi-objective function*. Tech. rep. 2019. URL: <https://upcommons.upc.edu/handle/2117/129389>.
- [15] Peng Hou et al. "A review of offshore wind farm layout optimization and electrical system design methods". In: *Journal of Modern Power Systems and Clean Energy* 7.5 (2019), pp. 975–986. DOI: [10.1007/s40565-019-0550-5](https://doi.org/10.1007/s40565-019-0550-5).

- [16] Himanshu J. Bahirat, Bruce A. Mork, and Hans Kr. Høidalen. "Comparison of wind farm topologies for offshore applications". In: *2012 IEEE Power and Energy Society General Meeting*. 2012, pp. 1–8. doi: [10.1109/PESGM.2012.6344689](https://doi.org/10.1109/PESGM.2012.6344689).
- [17] ABB. *XLPE Submarine Cable Systems Attachment to XLPE Land Cable Systems - User's Guide*. Tech. rep. 2019.
- [18] G. Andersson. "Modelling and Analysis of Electric Power Systems". In: Lecture 227-0526-00. ITET ETH Zürich, Zürich, 2008. Chap. 2.
- [19] EC 60287-1-1, *Electric cables - Calculation of the current rating - Part 1-1: Current rating equations (100 load factor) and calculation of losses - General*. Tech. rep. International Electrotechnical Commission, 2006.
- [20] Jordi-Roger Riba. "Analysis of formulas to calculate the AC resistance of different conductors' configurations". In: *Electric Power Systems Research* 127 (2015), pp. 93–100. issn: 0378-7796. doi: <https://doi.org/10.1016/j.epsr.2015.05.023>. url: <https://www.sciencedirect.com/science/article/pii/S0378779615001649>.
- [21] Christoph Kaufmann, Jovana Dakic, and Oriol Bellmunt. "Multi-objective Optimization of Cable Sizes of an Offshore Wind Power Plant Collector System". In: Oct. 2019.
- [22] Arthur R. Bergen. "Power systems analysis". eng. In: *Power systems analysis*. 2nd ed. Upper Saddle River, N.J: Prentice-Hall, 2000. Chap. 10, pp. 323–352. isbn: 0136919901.
- [23] Arthur R. Bergen. "Power systems analysis". eng. In: *Power systems analysis*. 2nd ed. Upper Saddle River, N.J: Prentice-Hall, 2000. Chap. 5,5, pp. 157–170. isbn: 0136919901.
- [24] M. Dicorato et al. "Guidelines for assessment of investment cost for offshore wind generation". In: *Renewable Energy* 36.8 (2011), pp. 2043–2051. issn: 0960-1481. doi: <https://doi.org/10.1016/j.renene.2011.01.003>. url: <https://www.sciencedirect.com/science/article/pii/S0960148111000097>.
- [25] Christoph Kost et al. *Levelized cost of electricity renewable energy technologies*. Tech. rep. FRAUNHOFER INSTITUTE FOR SOLAR ENERGY SYSTEMS ISE, 2021.
- [26] Stephan C. Carlson. *graph theory*. 2020. url: <https://www.britannica.com/topic/graph-theory>.
- [27] *Advances in Multi-Objective Nature Inspired Computing*. eng. 1st ed. 2010. Studies in Computational Intelligence, 272. Berlin, Heidelberg: Springer Berlin Heidelberg, 2010. isbn: 1-280-00335-9.
- [28] Artur M. Schweidtmann et al. "Machine learning meets continuous flow chemistry: Automated optimization towards the Pareto front of multiple objectives". In: *Chemical Engineering Journal* 352 (2018), pp. 277–282. issn: 1385-8947. doi: <https://doi.org/10.1016/j.cej.2018.07.031>. url: <https://www.sciencedirect.com/science/article/pii/S1385894718312634>.
- [29] Nyoman Gunantara. "A review of multi-objective optimization: Methods and its applications". In: *Cogent Engineering* 5.1 (2018). Ed. by Qingsong Ai, p. 1502242. doi: [10.1080/23311916.2018.1502242](https://doi.org/10.1080/23311916.2018.1502242). eprint: <https://doi.org/10.1080/23311916.2018.1502242>. url: <https://doi.org/10.1080/23311916.2018.1502242>.
- [30] *Intersection of Two Lines (line_intersection)*. 2022. url: https://github.com/tamaskis/line_intersection-MATLAB/releases/tag/v5.0.4 , %20GitHub . %20Retrieved%20June%2028 , %202022.
- [31] Huang Ling-ling et al. "Optimization of large-scale offshore wind farm electrical collection systems based on improved FCM". In: Jan. 2012, pp. 1–6. doi: [10.1049/cp.2012.1785](https://doi.org/10.1049/cp.2012.1785).
- [32] Siemens Gamesa. *SWT-7.0-154 Offshore wind turbine*. 2022. url: <https://www.siemensgamesa.com/en-int/products-and-services/offshore/wind-turbine-swt-7-0-154>.

A Substation positioning

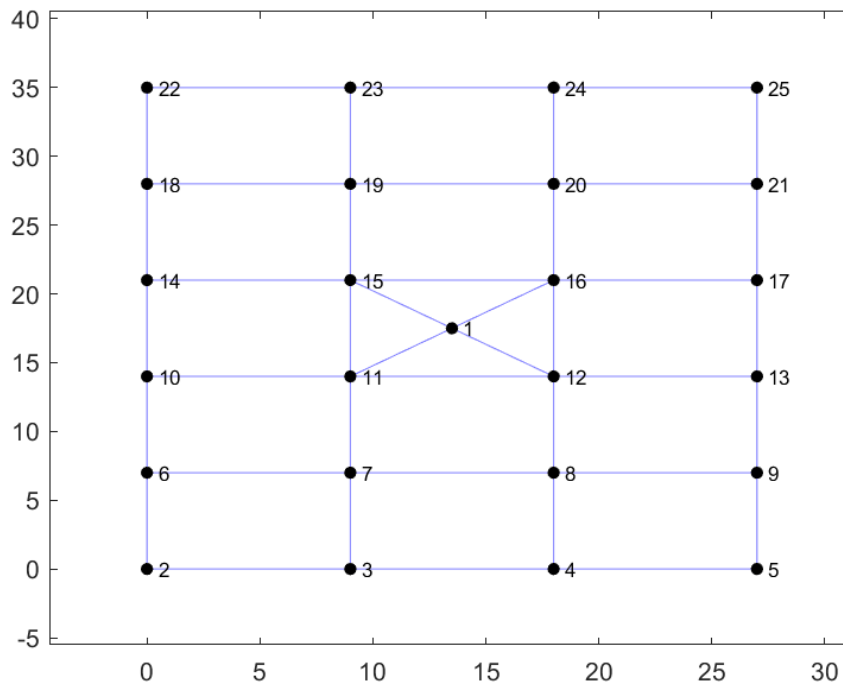


Figure 28: OWWP layout represented in a graph

Figure 28 represents the creation of the graph with all possible connections with the same limitations as the case study, only changing the location of the substation to $[13,5 \ 17,5]$. Figure 29 identifies the cable layout with shortest accumulative distance, which results in 26 304 m of cabling.

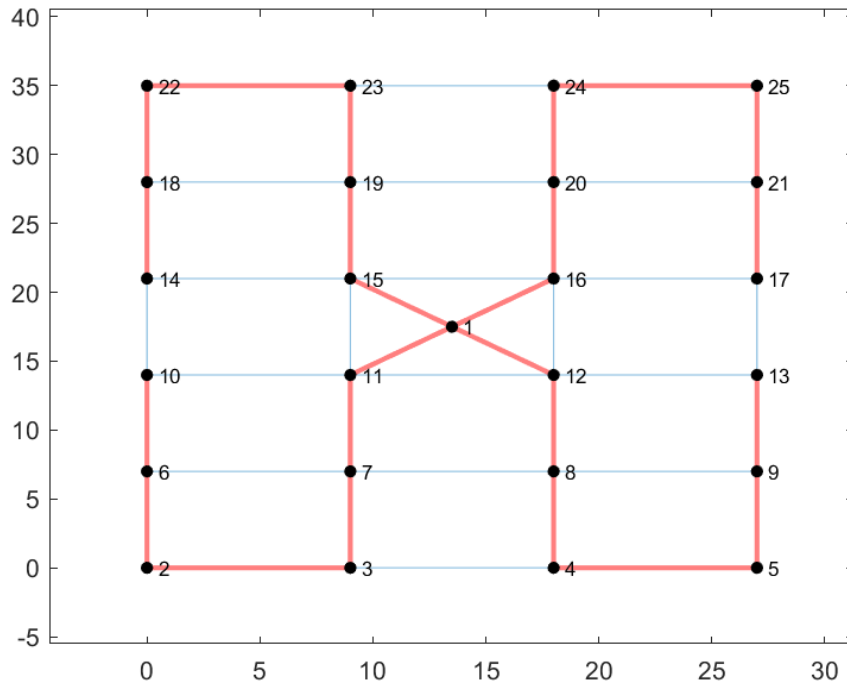


Figure 29: Least distance set up for cable distribution

B Increased number of possible collection system

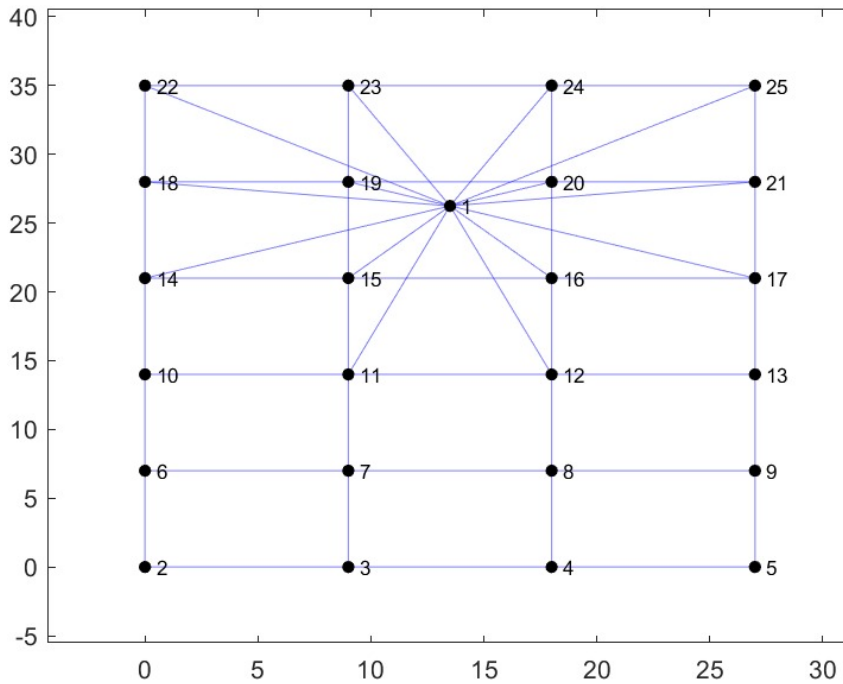


Figure 30: Cable possibilities with possible connections equal to 14

Figure 30 shows the graph generated with an increased possible connection equal to 9 instead of 4 as shown in the case study. For this iteration the MCDS had to be increased too. However, as shown in figure 31 the solution for the cabling is the same as the case study.

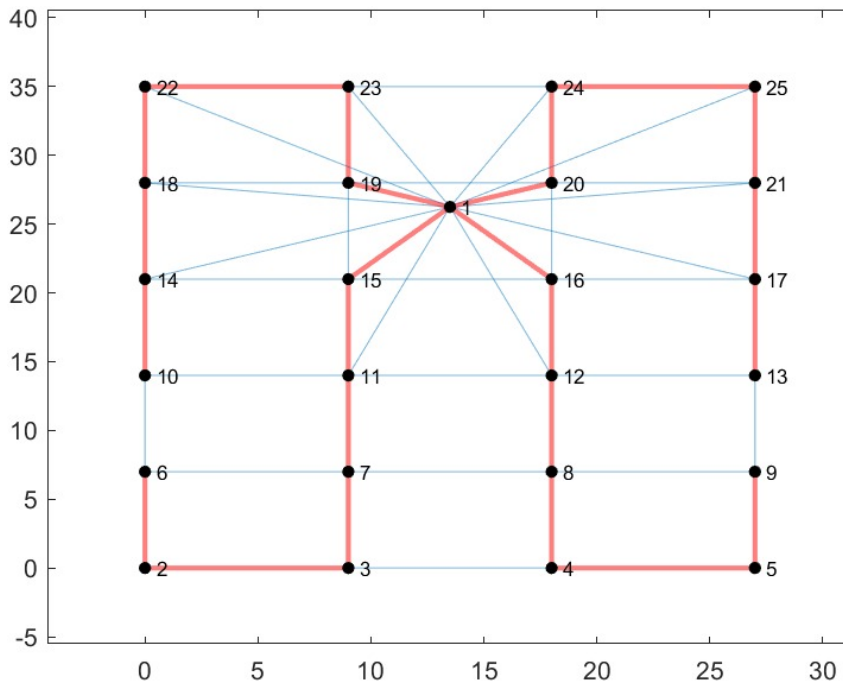


Figure 31: Solution of layout with increased possible connections

C Increased allowed distance between turbines

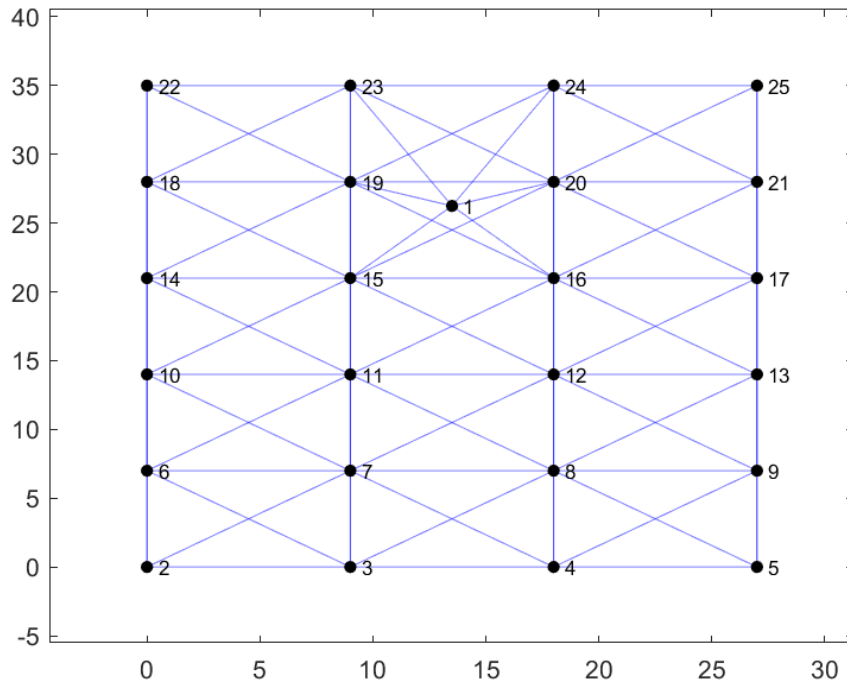


Figure 32: Cable possibilities with maximum allowed cabling distance equal to 15D